SCIENTIFIC REPORTS

OPEN

SUBJECT AREAS:
PALAEOCLIMATE
PALAEOCEANOGRAPHY

Received
6 December 2013

Accepted
5 June 2014

Published
27 June 2014

Correspondence and requests for materials should be addressed to J.N. (jnie@lzu.edu.cn)

* Current address: Department of Earth Sciences, University of Uppsala, Geocentrum, Villavägen 16 752 36 Uppsala, Sweden.

Pacific freshening drives Pliocene cooling and Asian monsoon intensification

Junsheng Nie[1], Thomas Stevens[2]*, Yougui Song[3], John W. King[4], Rui Zhang[1], Shunchuan Ji[1], Lisha Gong[1] & Danielle Cares[4]

[1]MOE Key Laboratory of Western China's Environmental Systems, Collaborative Innovation Centre for Arid Environments and Climate Change, Lanzhou University, Lanzhou 73000, China, [2]Centre for Quaternary Research, Department of Geography, Royal Holloway University of London, Egham, Surrey, TW20 0EX, UK, [3]State Key Laboratory of Loess and Quaternary Geology, Institute of Earth Environment, Chinese Academy of Sciences, Xi'an, P. O. Box 17, 710075, China, [4]Graduate School of Oceanography, University of Rhode Island, South Ferry Road, Narragansett, RI 02882, USA.

The monsoon is a fundamental component of Earth's climate. The Pliocene warm period is characterized by long-term global cooling yet concurrent monsoon dynamics are poorly known. Here we present the first fully quantified and calibrated reconstructions of separate Pliocene air temperature and East Asian summer monsoon precipitation histories on the Chinese Loess Plateau through joint analysis of loess/red clay magnetic parameters with different sensitivities to air temperature and precipitation. East Asian summer monsoon precipitation shows an intensified trend, paradoxically at the same time that climate cooled. We propose a hitherto unrecognized feedback where persistently intensified East Asian summer monsoon during the late Pliocene, triggered by the gradual closure of the Panama Seaway, reinforced late Pliocene Pacific freshening, sea-ice development and ice volume increase, culminating in initiation of the extensive Northern Hemisphere glaciations of the Quaternary Ice Age. This feedback mechanism represents a fundamental reinterpretation of the origin of the Quaternary glaciations and the impact of the monsoon.

The Pliocene (5.3–2.6 Ma) warm period, a possible analogue for future climate warming[1,2], is characterized by a global cooling trend culminating in the extensive Northern Hemisphere glaciations of the Quaternary (2.6–0 Ma)[3–6]. Recent work suggests that monsoon circulation intensifies over the same period[7–9]. However, this contradicts evidence that enhanced monsoons increase heat transport to high latitudes[10,11] as well as model predictions and geological records that show summer monsoons were generally weaker during colder periods[10,12,13]. Geochemical[7,8,14], magnetic[7,15] and biological[16–19] proxies have been widely used to infer summer monsoon history. A major problem inherent in these proxies is that they are potentially affected by both precipitation and temperature. During the Quaternary period when high (low) temperature was generally coupled with high (low) summer monsoon intensity[7,10] these proxies may be accurate in reflecting summer monsoon intensity. However, they cannot be assumed to show straightforward responses to monsoon intensity when temperature and precipitation potentially have different trends[7]. Therefore, significant debate[7,14,16,17,20] exists about Pliocene monsoon history. Understanding Pliocene monsoon history and its relationship with the onset of intensive Northern Hemisphere glaciations requires separation of precipitation and temperature signals.

Rock magnetic parameters are widely used in reconstructing paleoclimate history from aeolian sediments[7,15,21,22]. Magnetic susceptibility measured at 470 Hz (χ_{LF}) of surface soils across the Chinese Loess Plateau is strongly correlated with annual mean precipitation (AMP)[21,23]. Ultrafine magnetic grains with very high χ_{LF} but no stable magnetic remanence are produced via intermittent wetting and drying cycles associated with monsoon climate during soil formation on the Chinese Loess Plateau, and are responsible for high χ_{LF} in paleosol layers[21,23,24]. Fine stable single domain (SSD) and small pseudo- single domain (PSD) magnetic grains that have high anhysteretic remanent magnetization susceptibility (χ_{ARM}) but low χ_{LF} are also formed during soil formation[15]. Inter-parameter proxies for magnetic grain-size variations, such as χ_{ARM}/χ_{LF} and χ_{ARM}/SIRM, where SIRM represents saturated isothermal remanent magnetization and measures the magnetic grain concentration with remanence, are also sensitive paleoclimate indicators[15,24]. However, no study explores the relationship between magnetic parameter ratios and specific, separate climatic parameters for surface soils on the Chinese Loess Plateau.

Here we demonstrate that soil magnetic parameters have different sensitivities to AMP and annual mean temperature (AMT), based on a new surface soil calibration across the Chinese Loess Plateau (Fig. 1). Then, we use magnetic parameter records from wind-blown Pliocene red clay (finer and more weathered than Quaternary

loess) to discuss the evolution of paleotemperature and paleoprecipitation on the Chinese Loess Plateau. Finally, we tentatively present the first separate calibrated, quantitative reconstructions of Pliocene air temperature and East Asian summer monsoon precipitation history on the Chinese Loess Plateau through joint analysis of red clay magnetic parameters. Although these records have large uncertainties, this is the first quantified separation of these key aspects of Pliocene climate.

Results

Surface soil calibration. Fig. 2 shows the correlation patterns between Chinese Loess Plateau surface soil χ_{ARM}/χ_{LF} (Figs. 2a and 2b), χ_{ARM}/SIRM (Figs. 2c and 2d), χ_{ARM} (Figs. 2e and 2f), and AMP and AMT from meteorological stations closest to these surface soils (China Meteorological Data Sharing Service System: http://cdc.cma.gov.cn, in Chinese). We find that χ_{ARM}/SIRM is exponentially correlated with AMP and linearly correlated with AMT, as is the case for χ_{ARM}. The correlations of these two magnetic parameters with AMP are stronger than with AMT (Fig. 2 and Table 1). The correlation between χ_{ARM} and AMT is even weaker than the correlation between AMT and AMP, suggesting that χ_{ARM} is primarily controlled by AMP variations. By contrast, χ_{ARM}/χ_{LF} has similar R^2 values to AMP and AMT (Fig. 2a, 2b and Table 1). The correlation between χ_{ARM}/χ_{LF} and AMP is linear, whereas the correlation between χ_{ARM}/χ_{LF} and AMT is more complex with a concave down regression fit (Fig. 2a,2b and Table 1).

Paleoclimate reconstruction. The χ_{ARM}, χ_{ARM}/χ_{LF} and χ_{ARM}/SIRM records from Chaona[9] (35° 06′ N, 107° 12′ E) and Lingtai[25] (35° 04′ N, 107° 39′E), central Chinese Loess Plateau, covary with each other (Fig. 3). The three magnetic records co-vary from 6 to ~4.8 Ma. However, from ~4.3 to 2.7 Ma, the χ_{ARM} and χ_{ARM}/SIRM records show increasing trends while the χ_{ARM}/χ_{LF} record shows a decreasing trend.

Based on regression fits in Fig. 2f and 2h we tentatively reconstruct the first quantified temperature and precipitation history between 6 and 2.6 Ma on the Chinese Loess Plateau (Fig. 3f and 3g). χ_{ARM} is not sensitive to AMT variations and can therefore be used to estimate AMP history (Fig. 2f). Based on the correlation fit between χ_{ARM}/χ_{LF} and AMT × AMP (Fig. 2h) and the reconstructed AMP record (Fig. 2f) we then tentatively also reconstruct AMT history on the Chinese Loess Plateau for the interval 6–2.6 Ma. We also use χ_{ARM}/SIRM to estimate AMP (Fig. 2d), and then solve for AMT based on the correlation relationship between χ_{ARM}/χ_{LF} and AMT × AMP (Fig. 2h) and the reconstructed AMP record (Fig. 2d). The resultant AMP and AMT values between these two independent methods are closely aligned (Fig. 4), supporting the reconstructions.

Discussion

This concave down shaped regression fit between χ_{ARM}/χ_{LF} and AMT indicates that χ_{ARM}/χ_{LF} is more sensitive to temperature variations when temperature is lower. By contrast, the concave up shaped regression fits between χ_{ARM}/SIRM or χ_{ARM} and AMP indicates that χ_{ARM}/χ_{LF} and χ_{ARM} are more sensitive to precipitation variations when precipitation is higher (Table 1 and supplementary materials).

These relationships suggest that in the scenario of high (low) precipitation coupled with high (low) temperature, χ_{ARM}, χ_{ARM}/χ_{LF} and χ_{ARM}/SIRM should all have similar trends, with higher

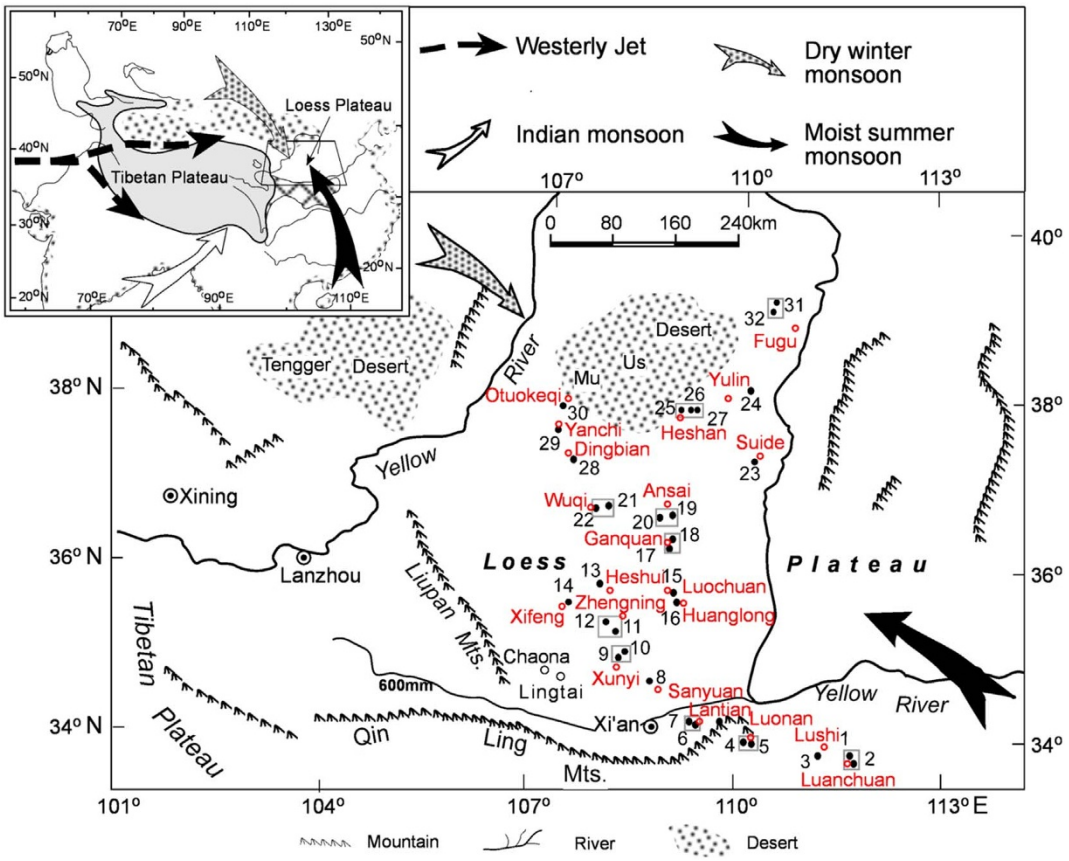

Figure 1 | Schematic map of the Chinese Loess Plateau and the location of the Chaona section (black circle), the Lingtai section (black circle), surface soil samples (solid dots) and meteorological stations (red circle) used in this paper. The inset illustrates the location of the Chinese Loess Plateau relative to the Tibetan Plateau and modern Asian atmospheric circulation. Magnetic parameter values were averaged for dots within the gray rectangle before comparing with the meteorological data closest to them. Revised from Song et al. (2007)[54].

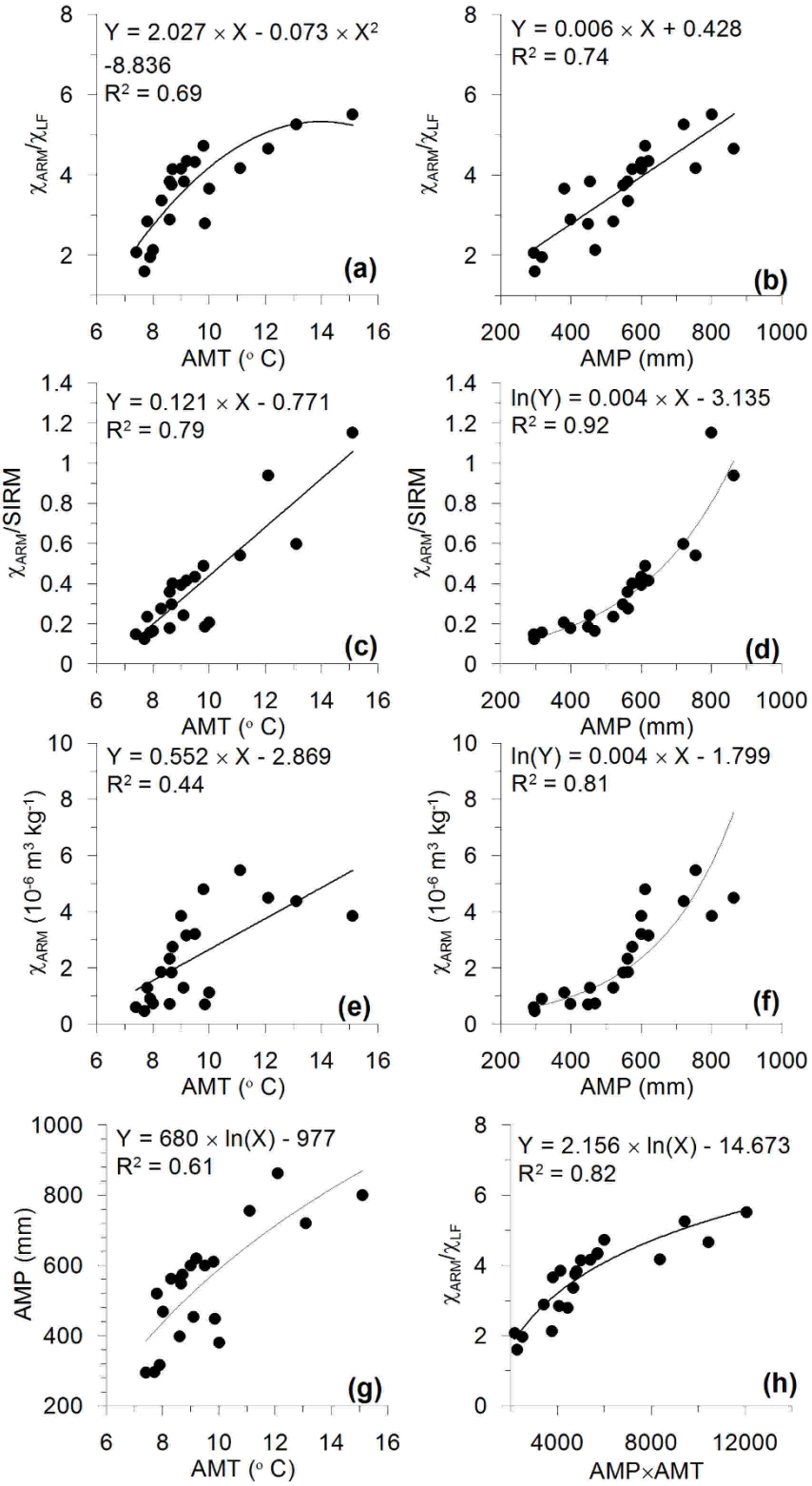

Figure 2 | Correlation patterns between Chinese Loess Plateau surface soil magnetic and climatic parameters. (a), χ_{ARM}/χ_{LF} and AMP; (b), χ_{ARM}/χ_{LF} and AMT; (c), χ_{ARM}/SIRM and AMP; (d), χ_{ARM}/SIRM and AMT; (e), χ_{ARM} and AMP; (f), χ_{ARM} and AMT; (g), AMP and AMT of meteorological stations closest to these surface soils; (h), χ_{ARM}/χ_{LF} and AMP × AMT. Meteorological data are from the China Meteorological Data Sharing Service System (http://cdc.cma.gov.cn, in Chinese).

(lower) magnetic parameter values corresponding to higher (lower) precipitation and temperature. This relationship has been shown to be the case in the Quaternary when precipitation and temperature are coupled[15]. However, χ_{ARM}/χ_{LF} and χ_{ARM}/SIRM should show different trends in the scenario of increasing precipitation and decreasing temperature trends, as has been speculated for the Pliocene[7]. In this case, χ_{ARM}/SIRM and χ_{ARM} will have an increasing trend, controlled dominantly by the effects of increasing precipitation (Fig. 2d, 2f and Table 1), while χ_{ARM}/χ_{LF} will have a decreasing trend, attributed to the dominant effects of decreasing temperature

Table 1 | Correlations between magnetic and climatic parameters

Parameter	R^2	Type of correlation	Sensitivity
χ_{ARM}/χ_{LF} (y axis), AMP (x axis)	0.74	Linear	No
χ_{ARM}/χ_{LF} (y axis), AMT (x axis)	0.69	Concave down, slope decreasing	Low Temperature variation
χ_{ARM}/SIRM (y axis), AMP (x axis)	0.92	Concave up, slope increasing	High precipitaiton variation
χ_{ARM}/SIRM (y axis), AMT (x axis)	0.79	Linear	No
χ_{ARM} (y axis), AMP (x axis)	0.81	Concave up, slope increasing	High precipitaiton variation
χ_{ARM} V(y axis), AMT (x axis)	0.44	Linear	No
AMP (y axis), AMT (x axis)	0.61	Concave down, slope decreasing	\

Note: AMP: annual mean precipitation; AMT: annual mean temperature.

(Fig. 2a and Table 1). However, any decreasing trend of χ_{ARM}/χ_{LF} should be modest because of the effects of increasing precipitation, which will tend to pull the decreasing χ_{ARM}/χ_{LF} trend in the opposite direction. For similar reasons, an increasing trend of χ_{ARM}/SIRM should also be modest because of the effects of decreasing temperature, which will tend to pull the increasing χ_{ARM}/SIRM trend in the opposite direction. In the scenario of increasing temperature and decreasing precipitation trends, χ_{ARM}/SIRM will have an increasing trend or stay at a constant low value, attributed to effects of decreasing precipitation; and χ_{ARM}/χ_{LF} will have a decreasing trend, attributed to effects of decreasing precipitation. However, the trends will again be modest because of the opposite effects of temperature and precipitation.

During ~4.8–6 Ma, the χ_{ARM}, χ_{ARM}/χ_{LF} and χ_{ARM}/SIRM records from Chaona and Lingtai co-vary with each other (Fig. 3a, b, and c) and with ice volume[26]. This relationship is consistent with the concept that monsoon climate dominated the Chinese Loess Plateau and high (low) temperature was coupled with high (low) precipitation[7]. However, during ~4.8–2.7 Ma, χ_{ARM}/χ_{LF} decreases but both the χ_{ARM} and χ_{ARM}/SIRM records increase (Fig. 3a, b, and c). Based on the above surface calibration results (Fig. 2 and Table 1), we conclude that the Chinese Loess Plateau experienced a cooling trend coeval with increasing precipitation from ~4.8 to 2.7 Ma. The quantitative reconstructions support the conclusion that the Chinese Loess Plateau experienced a cooling trend concomitant with increasing precipitation from ~4.8 to 2.7 Ma (Figs. 3f and g).

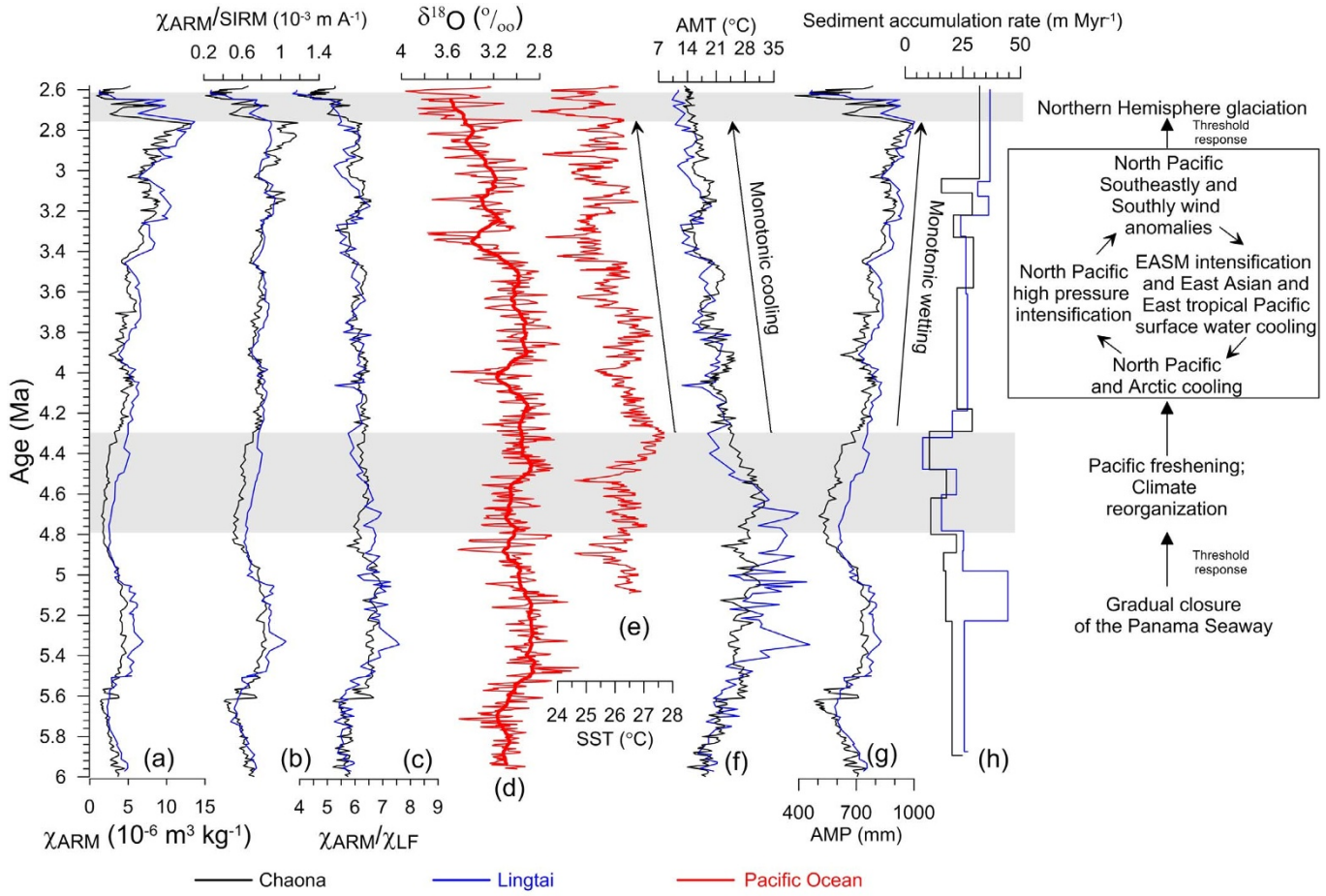

Figure 3 | Paleoclimatic and paleoceanographic data for the time interval 6–2.6 Ma. (a), (b), (c), the Chaona (black) and Lingtai (blue) χ_{ARM}, χ_{ARM}/SIRM and χ_{ARM}/χ_{LF} records, respectively. (d), (e), East Equatorial Pacific Ocean Drilling Project (ODP) site 846 benthic oxygen isotope[26] and sea surface temperature[6] records respectively. (f), (g), reconstructed Chaona (black) and Lingtai (blue) annual mean temperature (AMT) and annual mean precipitation (AMP) records based on the correlation regression fits in Figs. 2f and 2h respectively. (h), Chaona (black) and Lingtai (blue) sedimentation rate records. For the interval 3.6–2.6 Ma, the Chaona and Lingtai age models were tuned to the monsoon stack[55]; for the interval 6–3.6 Ma, the age models of the two sites are based on paleomagnetic dating[9,25]. EASM: East Asian summer monsoon.

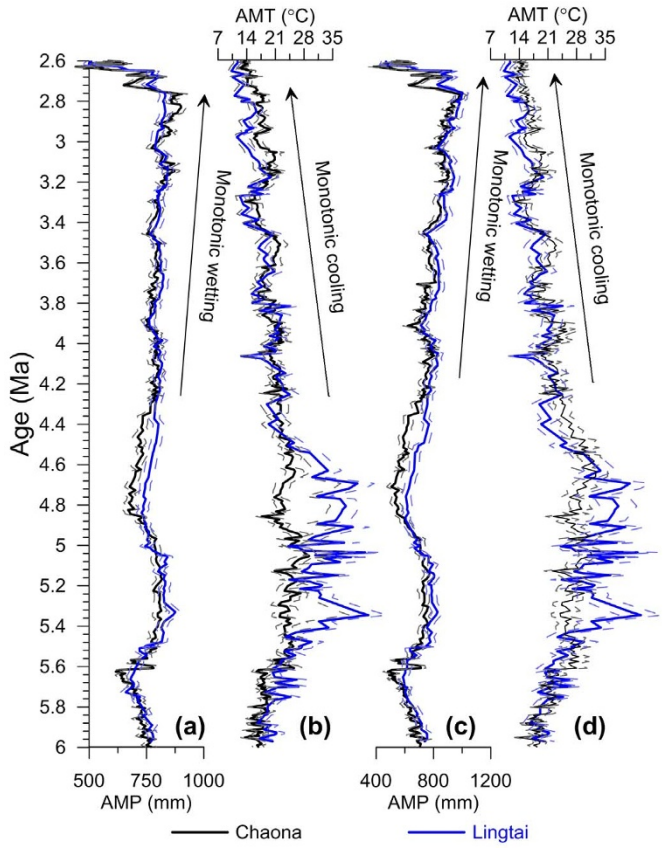

Figure 4 | A comparison of reconstructed annual mean precipitation (AMP) and annual mean temperature (AMT). (a), AMP based on the empirical relationship in Fig. 2d; (b), AMT based on the empirical relationships in Figs. 2d and 2h; (c), AMP based on the empirical relationship in Fig. 2f; (d), AMT based on the empirical relationships in Figs. 2f and 2h. We note that the AMT and AMP records based on two methods have similar trends. The dashed line represents the 2 σ uncertainty (standard error) of each record. The uncertainties in the paleo data were propagated from the uncertainties of surface soils in Fig. 2.

In contrast to the above, some biological and geochemical records[14,27] on the Chinese Loess Plateau have been used to suggest drying climate from ~4.5 to 2.7 Ma on the Chinese Loess Plateau. However, we argue that biological and geochemical proxies are influenced by both temperature and precipitation. Furthermore, pollen records from the Chaona section[19,28] are consistent with our inferences based on magnetic parameters. According to these studies, during the late Pliocene, *Cupressaceae* and *Juniperus* along with *Ulmus* dominated the Loess Plateau, revealing that the environment showed a marked change characterized by hot and rainy summers and cold and dry winters[19,28]. This inconsistency between biological records on the Loess Plateau[19,27] underscores the complexity of using biological evidence to infer monsoon intensity. Geochemical monsoon records, such as the widely used Chemical Index of Alternation, suggest that chemical weathering was weaker on the Loess Plateau during the late Pliocene in comparison with the early Pliocene. However, geochemical parameters are affected not only by precipitation, but also by temperature (controlling reaction rates) and materials available to weather (determined by sediment accumulation rate)[29]. It is widely reported that sediment accumulation rate is higher for the late Pliocene on the Loess Plateau[14,30] (Fig. 3h), leading to more materials available for weathering. Thus, weaker chemical weathering and alteration is not necessarily linked with weaker monsoon precipitation, but can be attributed to cooler climate and the availability of sediment for weathering[14] (Fig. 3h). Our magnetic evidence does not suffer from these ambiguities and demonstrates increased precipitation over this period.

While the general qualitative trends in our data are clear, and similar trends are seen in the quantitative data, our quantitative reconstructions potentially have large uncertainties. First, although magnetic parameters have different sensitivities to AMP and AMT, each of them is potentially affected in part by both AMP and AMT. Thus, the influence of another component cannot be entirely removed, even if the majority of variation can be explained by one climate parameter alone. Second, the reconstructed Pliocene paleotemperature exceeds modern temperatures on the Chinese Loess Plateau. Although it is well known that the Pliocene was warmer than the Quaternary[31], these higher temperatures increase the uncertainties associated with the quantitative paleotemperature reconstructions based on our modern climofunction during the Pliocene. Third, the decoupled temperature and precipitation trends on the Chinese Loess Plateau seem to contrast with proposed monsoonal climate in the region, potentially meaning that modern monsoonal analogues cannot be directly applied to Pliocene red clay. However, although our records show that Pliocene temperature and precipitation on the Loess Plateau have opposite trends over tectonic timescales, it is clear from our records (Fig. 3) that at orbital timescales, temperature and precipitation are in phase, consistent with features of a monsoonal climate[32]. Thus, we maintain that modern calibrations can still be used to understand Pliocene magnetic paleoclimatic records.

This method used here is readily applicable to loess or red clay where magnetic enhancement occurred during interglacial periods associated with increases in abundance of ultrafine magnetic grains produced via soil-formation processes[33,34]. However, caution needs to be exercised in situations where magnetic minerals tend to be destroyed during soil-formation processes, such as in Siberian or Argentine loess[35–37].

The interval during ~4.8–4.3 Ma has been argued to be anomalous on the Chinese Loess Plateau[20]. Abundant clay coatings and a high free iron/total iron ratio in red clay sediments suggest that this interval experienced high monsoon precipitation[20]. However, by contrast this interval shows low χ_{LF} values[7,20]. Thus, it has been argued that χ_{LF} is not able to indicate East Asian Summer Monsoon intensity for this time interval[20]. However, we note that, in contrast to any other time interval during 6–2.6 Ma, ~4.8–4.3 Ma is dominated by low sedimentation rate (Fig. 3h) giving a significantly longer time for soils to develop clay coatings and experience chemical weathering. In contrast, magnetic enhancement of Chinese loess is not a function of pedogenic duration[21] and magnetic parameters will thus better reflect climate conditions during this time period. Lower dust sedimentation rates can therefore explain the inconsistent monsoon proxies during ~4.8–4.3 Ma on the Chinese Loess Plateau. This time interval is synchronous with the point when the gradual closure of the Panama Seaway started to significantly affect surface seawater exchange between the Equatorial Pacific Ocean and the Caribbean Sea[38] and signals initiation of Northern Hemisphere climate reorganization (Fig. 3).

There are two potential ways to explain the Pliocene wetting trend on the Chinese Loess Plateau: intensified East Asian summer monsoon precipitation or intensified westerly precipitation. However, oceanic moisture sources for westerly flow are far away from the Chinese Loess Plateau, limiting the contribution from westerly precipitation. We have previously attributed an apparently intensified East Asian Summer Monsoon simultaneous with increasing ice volume from 4.7 to 2.6 Ma to the combined effects of the closure of the Panama Seaway and Tibetan plateau uplift[9]. However, evidence supporting late Pliocene uplift of the Tibetan plateau is controversial[39] and attempts to separate temperature and precipitation trends have not been performed. Here we propose an alternative

mechanism to explain concurrent Pliocene climate cooling and monsoon intensification, demonstrated from the magnetic parameter records having different sensitivities to AMT and AMP. Paleoceanographic data[38] show that as a result of gradual closure of the Panama Seaway, East Equatorial Pacific surface water freshens from ~4.8 Ma due to easterly trade wind transportation of moisture from the central Atlantic Ocean and the Caribbean Sea to the tropical Pacific Ocean. Modern day salinity differences between the East Equatorial Pacific Ocean and the Caribbean Sea[38] were established by ~4.2 Ma. Fresher seawater will then have been transported to the North Pacific Ocean via ocean currents surrounding the North Pacific gyre, causing freshening of the North Pacific surface water. This freshening drove enhanced sea ice formation on the surface North Pacific[40]. Model simulation[41] demonstrates that sea ice formation would strengthen the high pressure center over the North Pacific, enhancing Southerly and Southeasterly winds, which in turn would intensify East Asian Summer Monsoon precipitation and meridional moisture transport[41] (Supplementary Fig. 1). Critically, we propose that intensified meridional moisture transport would cause further middle and high latitude precipitation (Fig. 3) and consequent further freshening in the Pacific and the Arctic Oceans. This change would drive additional intensification of the North Pacific high pressure center and East Asian Summer Monsoon precipitation[41]. We note that this meridionally-transported moisture would likely also have been transported to the North American continent[2], providing a moisture source for North American ice sheets to grow. This previously unknown positive feedback explains for the first time the paradox of concurrent Pliocene cooling and East Asian Summer Monsoon precipitation intensification. Our hypothesis also explains previous paleoceanographic data[6] that reveal that East Equatorial Pacific surface water experienced a cooling trend from ~4.3 to 2.6 Ma (Fig. 4e). No corresponding forcing was identified but under our proposed feedback an intensified North Pacific high pressure system at the same time would drive Equatorial Pacific water flow from east to west, intensifying upwelling and providing a reasonable explanation for the observed East Equatorial cooling trend. This previously overlooked positive feedback was initiated in the run up to the onset of extensive Northern Hemisphere glaciation. As it forces gradual cooling of Pacific surface water while at the same time providing both a moisture source for ice sheets and a freshwater driver for sea ice growth, we argue that this Pacific atmosphere-ocean feedback is a critical but hitherto unrecognized factor in the initiation of the Northern Hemisphere glaciation of the Quaternary Ice Age.

The model simulation of reference 41 is an important basis for our hypothesis. However, one important difference exists between the two studies. Reference 41 presents climate during boundary condition snapshots: completely closed and open (with sill depth of 2559 m) Panama Seaway. By contrast, our hypothesis treats the seaway closure as a continuous process, decreasing sill depth[42] from probably less than 200 to 0 m. Using a sill depth close to that of the Pliocene (370 m), a study[43] found that closure of the Panama Seaway would intensify precipitation in Northern Hemisphere high latitudes but that this closure plays a limited role in initiation of the Northern Hemisphere glaciations. However, reference 43 did not include the new positive feedback involving monsoon intensification proposed in this paper.

Reference 41 produces a weakened East Asian winter monsoon associated with closure of the Panama Seaway and development of a high pressure system over the North Pacific Ocean. This contrasts with evidence demonstrating that the East Asian winter monsoon became stronger during the late Pliocene[7]. We note that although reference 41 showed geographical distribution of surface air pressure and wind during February which includes the information of Siberian-Mongolian high pressure system, it did not consider the likely intensification of the Siberian-Mongolian high pressure system from the early to the late Pliocene under global cooling[44,45]. As this system has more direct control over the winter climate on the Chinese Loess Plateau, due to its proximity, this explains the inconsistency between the model simulation results of reference 41 and the geological observations[7].

A recent study[46] also reported that different models produced variable sea surface salinity changes associated with closure of the Panama Seaway. However, only three of the 12 models (EC(415 m); CCMS3(1475 M); UVIC 6sh(130 m)) show dominantly increasing sea surface salinity associated with closure of the Panama Seaway. More importantly, of the 12 models examined, only the HacCM3 model by reference 43 used boundary conditions representative of part of the Pliocene. Thus, the results of reference 43, which demonstrated that the North Pacific sea surface salinity decreased significantly associated with closure of the Panama Seaway, are more convincing as accurate representations of Pliocene salinity.

While the closure of the Panama seaway is well constrained in the Pliocene, whether the Tibetan Plateau experienced a phase of intense uplift during the Pliocene is a topic of long-standing debate[44,47–50]. No clear phase of intensive uplift is known for 4.6 Ma and although some model simulations demonstrate the potential climatic influence of the plateau[7,51], our reconstructions demonstrate the close association of Pliocene climate change with closure of the Panama seaway. A permanent Pliocene El Niño condition has been hypothesized to exist in the Pacific Ocean, possibly associated with closure of the Indonesian Seaway, while the end of this condition around 2.7 Ma may have contributed to initiation of the intensive Northern Hemisphere glaciations[52]. However, a recent study based on a coupled atmosphere-ocean general circulation model demonstrates that were the Pliocene dominated by a permanent El Niño-like condition it is unlikely that this would provide a major contribution to global warmth and its termination cannot contribute significantly to the onset of the intensive Northern Hemisphere glaciations[53]. Indeed, this same simulation found that there was no permanent El Niño-like condition during the Pliocene[53].

As such, the Panama seaway closure initiated positive feedback involving monsoon circulation provides the best explanation of the data here. This paper demonstrates the fundamental importance of a hitherto unknown oceanographic-atmospheric feedback in driving late Cenozoic cooling, monsoon intensification and the onset of Northern Hemisphere glaciation, initiated by tectonic forcing. Our explanation of Pliocene climate trends emphasizes the Pacific as central to global climate. Model simulations[1,2] of Pliocene and future climate need to take account of this hitherto unknown mechanism.

Methods

Surface soil samples were taken ~1 cm below the surface from A-horizons at locations across the Chinese Loess Plateau (Fig. 1). Removing the top 1 cm removes the potential effects of pollution to these soils. In selecting sites, we sought level, stable land surfaces that showed no obvious evidence of surface erosion or extensive human disturbance.

For all samples, magnetic susceptibility was measured using a Bartington MS2 susceptometer at frequencies of 470 Hz (i.e., χ_{LF}) and 4700 Hz (i.e., χ_{HF}). For surface soils and Chaona samples ARM was imparted using a 100 mT peak AF and a 0.05 mT constant biasing field, while for Lingtai samples ARM was imparted using a 100 mT peak AF and a 0.1 mT constant biasing field. This parameter is also expressed as χ_{ARM} after normalization by the 0.05/0.1 mT direct bias field. SIRM was imparted in all samples at 1 T using a pulse magnetizer and measured using a 2 G cryogenic magnetometer on Chaona and surface samples, and using a spinner magnetometer for Lingtai samples. Following these measurements, χ_{ARM}/χ_{LF} and χ_{ARM}/SIRM were calculated.

Because of the different bias field used for the Chaona and Lingtai samples when acquiring ARM, it is not feasible to compare the absolute magnetic parameter values directly. The highest χ_{ARM} values at Lingtai and Chaona between 6 and 2.6 Myr are 16.753 and 13.164 ($\times 10^{-6}$ m^3 kg^{-1}) respectively, both occurring at ~2.76 Myr. As such, we divide the Lingtai χ_{ARM}, χ_{ARM}/χ_{LF} and χ_{ARM}/SIRM records by 16.753/13.164 (=1.273) to correct the bias field effects and to allow direct comparison of magnetic records from both sections. The corrected Lingtai magnetic records

correlate well with the records from Chaona (Fig. 3a, b, and c), demonstrating that the above correction is valid.

1. Dowsett, H. J. *et al.* Assessing confidence in Pliocene sea surface temperatures to evaluate predictive models. *Nature Clim. Change* **2**, 365–371, doi:10.1038/nclimate1455 (2012).
2. Lunt, D. J., Foster, G. L., Haywood, A. M. & Stone, E. J. Late Pliocene Greenland glaciation controlled by a decline in atmospheric CO_2 levels. *Nature* **454**, 1102–1105, doi:10.1038/nature07223 (2008).
3. Lisiecki, L. & Raymo, M. E. Plio-Pleistocene climate evolution: Trends and transitions in glacial cycle dynamics. *Quat. Sci. Rev.* **26**, 56–69 (2007).
4. Ravelo, A. C., Andreasen, D. H., Lyle, M., Olivarez Lyle, A. & Wara, M. W. Regional climate shifts caused by gradual cooling in the Pliocene epoch. *Nature* **429**, 263–267 (2004).
5. Fedorov, A. V. *et al.* The Pliocene Paradox (Mechanisms for a Permanent El Nino). *Science* **312**, 1485–1489, doi:10.1126/science.1122666 (2006).
6. Lawrence, K., Liu, Z. & Herbert, T. Evolution of the Eastern Tropical Pacific Through Plio-Pleistocene Glaciation. *Science* **312**, 79–83 (2006).
7. An, Z. S., Kutzbach, J. E., Prell, W. L. & Porter, S. C. Evolution of Asian monsoons and phased uplift of the Himalaya-Tibetan plateau since Late Miocene times. *Nature* **411**, 62–66 (2001).
8. Clift, P. D. *et al.* Correlation of Himalayan exhumation rates and Asian monsoon intensity. *Nat. Geosci.* **1**, 875–880, doi:10.1038/ngeo351 (2008).
9. Nie, J., Song, Y., King, J. W., Zhang, R. & Fang, X. Six million years of magnetic grain-size records reveal that temperature and precipitation were decoupled on the Chinese Loess Plateau during ~4.5–2.6 Ma. *Quat. Res.* **79**, 465–470, doi:http://dx.doi.org/10.1016/j.yqres.2013.01.002 (2013).
10. Wang, Y. J. *et al.* A high-resolution absolute-dated Late Pleistocene monsoon record from Hulu Cave, China. *Science* **294**, 2345–2348, doi:10.1126/science.1064618 (2001).
11. Emile-Geay, J. *et al.* Warren revisited: Atmospheric freshwater fluxes and "Why is no deep water formed in the North Pacific" *J. Geophys. Res.* **108**, doi:10.1029/2001JC001058 (2003).
12. Prell, W. L. & Kutzbach, J. E. Monsoon variability over the past 150,000 years. *J. Geophys. Res.* **92**, 8411–8425, doi:10.1029/JD092iD07p08411 (1987).
13. An, Z. S. *et al.* Glacial-Interglacial Indian Summer Monsoon Dynamics. *Science* **333**, 719–723, doi:10.1126/science.1203752 (2011).
14. Ge, J. *et al.* Major changes in East Asian climate in the mid-Pliocene: Triggered by the uplift of the Tibetan Plateau or global cooling? *J. Asian Earth Sci.* **69**, 48–59, doi:http://dx.doi.org/10.1016/j.jseaes.2012.10.009 (2013).
15. Bloemendal, J. C. & Liu, X. Rock magnetism and geochemistry of two plio-pleistocene Chinese loess-paleosol sequences-implications for quantitative palaeoprecipitation reconstruction. *Palaeogeogr. Palaeoclimatol. Palaeoecol.* **226**, 149–166 (2005).
16. Wu, N. *et al.* Marked ecological shifts during 6.2–2.4 Ma revealed by a terrestrial molluscan record from the Chinese Red Clay Formation and implication for palaeoclimatic evolution. *Palaeogeogr. Palaeoclimatol. Palaeoecol.* **233**, 287–299 (2006).
17. Passey, B. H. *et al.* Strengthened East Asian summer monsoons during a period of high-latitude warmth? Isotopic evidence from Mio-Pliocene fossil mammals and soil carbonates from northern China. *Earth Planet. Sci. Lett.* **277**, 443–452 (2009).
18. Wang, L. *et al.* Palynological evidence for Late Miocene-Pliocene vegetation evolution recorded in the red clay sequence of the central Chinese Loess Plateau and implication for palaeoenvironmental change. *Palaeogeogr. Palaeoclimatol. Palaeoecol.* **241**, 118–128, doi:http://dx.doi.org/10.1016/j.palaeo.2006.06.012 (2006).
19. Ma, Y. *et al.* Chaona pollen records from 8.1-2.6 Ma in the central Chinese Loess Plateau. *Chin. Sci. Bull.* **50**, 1627–1635 (2005).
20. Ding, Z. L., Yang, S. L., Sun, J. M. & Liu, T. S. Iron geochemistry of loess and red clay deposits in the Chinese Loess Plateau and implications for long-term Asian monsoon evolution in the last 7.0 Ma. *Earth Planet. Sci. Lett.* **185**, 99–109 (2001).
21. Maher, B. & Hu, M. A high-resolution record of Holocene rainfall variations from the western Chinese Loess Plateau: antiphase behaviour of the African/Indian and East Asian summer monsoons. *The Holocene* **16**, 309–319 (2006).
22. Heslop, D., Langereis, C. G. & Dekkers, M. J. A new astronomical timescale for the loess deposits of Northern China. *Earth Planet. Sci. Lett.* **184**, 125–139 (2000).
23. Heller, F. *et al.* Quantitative estimates of pedogenic ferromagnetic mineral formation in Chinese loess and paleoclimatic implications. *Earth Planet. Sci. Lett.* **114**, 385–390. (1993).
24. Zhou, L., Oldfield, F., Wintle, A., Robinson, S. & Wang, J. T. Partly pedogenic origin of magnetic variations in Chinese loess. *Nature* **346**, 737–739 (1990).
25. Hu, X.-F., Xu, L.-F., Pan, Y. & Shen, M.-N. Influence of the aging of Fe oxides on the decline of magnetic susceptibility of the Tertiary red clay in the Chinese Loess Plateau. *Quat. Int.* **209**, 22–30, doi:http://dx.doi.org/10.1016/j.quaint.2009.02.019 (2009).
26. Shackleton, N. J., Hall, M. A. & Pate, D. in *Proc. Ocean Drill. Sci. Results* Vol. 138 eds Pisias, N. G., Janacek, L. A., Palmer-Julson, A. & Van Andel, T. H.) 337–355 (1995).
27. Wang, L. *et al.* Palynological evidence for Late Miocene–Pliocene vegetation evolution recorded in the red clay sequence of the central Chinese Loess Plateau and implication for palaeoenvironmental change. *Palaeogeogr. Palaeoclimatol. Palaeoecol.* **241**, 118–128 (2006).
28. Wu, F. *et al.* Plio-Quaternary stepwise drying of Asia: Evidence from a 3-Ma pollen record from the Chinese Loess Plateau. *Earth Planet. Sci. Lett.* **257**, 160–169, doi:http://dx.doi.org/10.1016/j.epsl.2007.02.029 (2007).
29. Clift, P. D., Wan, S. & Blusztajn, J. Reconstructing chemical weathering, physical erosion and monsoon intensity since 25 Ma in the northern South China Sea: A review of competing proxies. *Earth Sci. Rev.* **130**, 86–102, doi:http://dx.doi.org/10.1016/j.earscirev.2014.01.002 (2014).
30. Sun, D. H., Shaw, J., An, Z. S., Chen, M. & Yue, L. Magnetostratigraphy and paleoclimatic interpratation of a continuous 7.2 Ma Late Cenozoic eolian sediments from the Chinese Loess Plateau. *Geophys. Res. Lett.* **25**, 85–88 (1998).
31. Zachos, J., Pagani, M., Sloan, L., Thomas, E. & Billups, K. Trends, Rhythms, and Aberrations in Global Climate 65 Ma to Present. *Science* **292**, 686–693 (2001).
32. An, Z. The history and variability of the East Asian paleomonsoon climate. *Quat. Sci. Rev.* **19**, 171–187 (2000).
33. Maher, B. A., Alekseev, A. & Alekseeva, T. Magnetic mineralogy of soils across the Russian Steppe: climatic dependence of pedogenic magnetite formation. *Palaeogeogr. Palaeoclimatol. Palaeoecol.* **201**, 321–341 (2003).
34. Orgeira, M. J., Egli, R. & Compagnucci, R. H. in *The Earth's Magnetic Interior* Vol. 1 eds Petrovsky, E., Ivers, D., Harinarayana, T. & Herrero-Bervera, E.) 361–397 (Springer, 2011).
35. Heil, C. W., King, J. W., Zárate, M. A. & Schultz, P. H. Climatic interpretation of a 1.9 Ma environmental magnetic record of loess deposition and soil formation in the central eastern Pampas of Buenos Aires, Argentina. *Quat. Sci. Rev.* **29**, 2705–2718 (2010).
36. Liu, X. M., Hesse, P., Beget, J. & Rolph, T. Pedogenic destruction of ferrimagnetics in Alaskan loess deposits. *Aust. J. Soil Res.* **39**, 99–115 (2001).
37. Carter-Stiglitz, B., Banerjee, S. K., Gourlan, A. & Oches, E. A multi-proxy study of Argentina loess: Marine oxygen isotope stage 4 and 5 environmental record from pedogenic hematite. *Palaeogeogr. Palaeoclimatol. Palaeoecol.* **239**, 45–62, doi:10.1016/j.palaeo.2006.01.008 (2006).
38. Haug, G. H., Tiedemann, R., Zahn, R. & Ravelo, A. C. Role of Panama uplift on oceanic freshwater balance. *Geology* **29**, 207–210 (2003).
39. Molnar, P., Boos, W. R. & Battisti, D. S. Orographic Controls on Climate and Paleoclimate of Asia: Thermal and Mechanical Roles for the Tibetan Plateau. *Annu. Rev. Earth Planet. Sci.* **38**, 77–102, doi:10.1146/annurev-earth-040809-152456 (2010).
40. Driscoll, N. W. & Haug, G. H. A short circuit in thermohaline circulation: A cause for northern hemisphere glaciation? *Science* **282**, 436–438 (1998).
41. Motoi, T. & Chan, W.-L. Colder Subarctic Pacific with larger sea ice caused by closure of the Central American Seaway and its influence on the East Asian monsoon: a climate model study. *Geol. Soc., London, Spec. Pub.* **342**, 265–277, doi:10.1144/sp342.15 (2010).
42. Schmidt, D. in *Deep-Time Perspectives on Climate Change: Marrying the Signal from Computer Models and Biological Proxies* eds Williams, M., Haywood, A., Gregory, F. & Schmidt, D.) 429–444 (The Micropalaeontological Society, 2007).
43. Lunt, D. J., Valdes, P. J., Haywood, A. & Rutt, I. C. Closure of the Panama Seaway during the Pliocene: implications for climate and Northern Hemisphere glaciation. *Climate Dynam.* **30**, 1–18 (2008).
44. An, Z. *et al.* Eolian evidence from the Chinese Loess Plateau: the onset of the Late Cenozoic Great Glaciation in the Northern Hemisphere and Qinghai-Xizang Plateau uplift forcing. *Sci. Chin. (D)* **42**, 258–271, doi:10.1007/bf02878963 (1999).
45. Ding, Z. L., Derbyshire, E., Yang, S. L., Sun, J. M. & Liu, T. S. Stepwise expansion of desert environment across northern China in the past 3.5 Ma and implications for monsoon evolution. *Earth Planet. Sci. Lett.* **237**, 45–55, doi:http://dx.doi.org/10.1016/j.epsl.2005.06.036 (2005).
46. Zhang, X. *et al.* Changes in equatorial Pacific thermocline depth in response to Panamanian seaway closure: insights from a multi-model study. *Earth Planet. Sci. Lett.* **317**, 76–84 (2012).
47. Rea, D. K., Snoeckx, H. & Joseph, L. H. Late Cenozoic eolian deposition in the North Pacific: Asian drying, Tibetan uplift, and cooling of the northern hemisphere. *Paleoceanography* **13**, 215–224 (1998).
48. Fang, X. M. *et al.* Magnetostratigraphy of the late Cenozoic Laojunmiao anticline in the northern Qilian Mountains and its implications for the northern Tibetan Plateau uplift. *Sci. Chin. (D)* **48**, 1040–1051 (2005).
49. Zhang, P., Molnar, P. & Downs, W. R. Increased sedimentation rates and grain sizes 2-4 Myr ago due to the influence of climate change on erosion rates. *Nature* **410**, 891–897 (2001).
50. Molnar, P. & England, P. Late Cenozoic uplift of mountain ranges and global climate change: chicken or egg? *Nature* **346**, 29–34 (1990).
51. Zhang, R., Jiang, D., Liu, X. & Tian, Z. Modeling the climate effects of different subregional uplifts within the Himalaya-Tibetan Plateau on Asian summer monsoon evolution. *Chin. Sci. Bull.* **57**, 4617–4626, doi:10.1007/s11434-012-5284-y (2012).
52. Cane, M. A. & Molnar, P. Closing of the Indonesian seaway as a precursor to east African aridification around 3? million years ago. *Nature* **411**, 157–162 (2001).
53. Haywood, A., Valdes, P. & Peck, V. A permanent El Nino-like state during the Pliocene? *Paleoceanography* **22**, doi:10.1029/2006PA001323 (2007).
54. Song, Y. *et al.* Late Neogene rock magnetic record of climatic variation from Chinese eolian sediments related to uplift of the Tibetan Plateau. *J. Asian Earth Sci.* **30**, 324–332 (2007).

55. Sun, Y., Clemens, S. C., An, Z. S. & Yu, Z. Astronomical timescale and palaeoclimatic implication of stacked 3.6-Myr monsoon records from the Chinese Loess Plateau. *Quat. Sci. Rev.* **25**, 33–48 (2006).

Acknowledgments

We thank the editor M. Meinshausen and three reviewers for thorough and constructive reviews. We thank S. Qin for assistance in uncertainty estimation of the paleoprecipitation and paleotemperature data and X. Hu for sharing Lingtai data. This work was jointly funded by the (973) National Basic Research Program of China (Grant No. 2013CB956400), the Strategic Priority Research Program of the Chinese Academy of Sciences (Grant No. XDB03020400), the National Natural Science Foundation (Grant Nos. 41172329; 41372036; 41321061; 41021091), the Research Fund for the Doctoral Program of Higher Education of China (Grant No. 20110211110012), and the Fundamental Research Funds for the Central Universities.

Author contributions

J.N., T.S., J.K. and Y.S. designed the research and J.N. and T.S. wrote the main manuscript text. J.N., R.Z., S.J., L.G., C.D. and Y.S. performed the experiments. All authors reviewed the manuscript.

Additional information

Supplementary information accompanies this paper at http://www.nature.com/scientificreports

Competing financial interests: The authors declare no competing financial interests.

How to cite this article: Nie, J. *et al.* Pacific freshening drives Pliocene cooling and Asian monsoon intensification. *Sci. Rep.* **4**, 5474; DOI:10.1038/srep05474 (2014).